Chapter 43 - SANS FROM CRYSTALLINE LAMELLAE

Polymers with regular structures can crystallize whether in solution or in the melt state. Solution crystallization forms regular lamellar structures and is the focus here. Crystalline lamellae qualify for inclusion in this part on "self-assembling systems".

1. A CRYSTALLINE POLYMER SOLUTION

Scattering from poly(ethylene oxide) (PEO) in d-ethanol (deuterated ethanol) solutions shows a strong low-Q SANS signal at low temperatures (below 40 ^{o}C). A low-Q, SANS signal could be due to many effects including aggregation, clustering, phase separation, crystallization or just undesired bubbles in the sample.

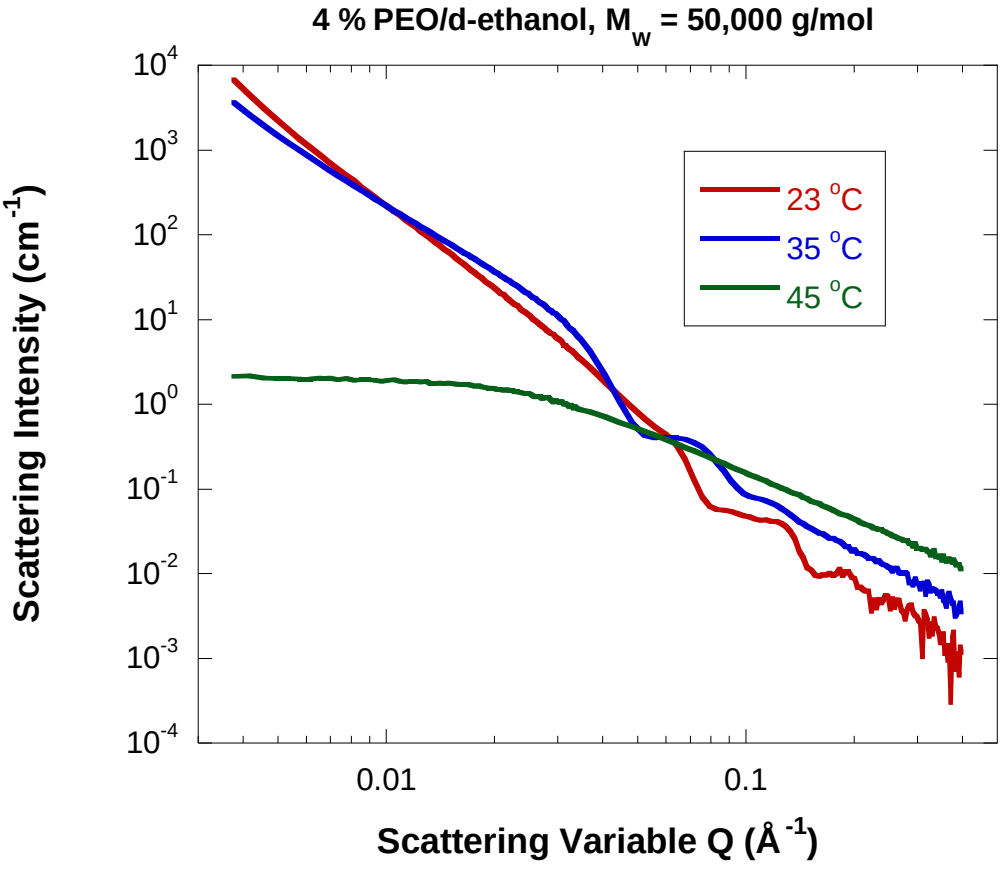

Figure 1: SANS from 4 % PEO/d-ethanol (mass fraction) measured at temperatures below and above the crystal melting temperature. The incoherent background component has been subtracted.

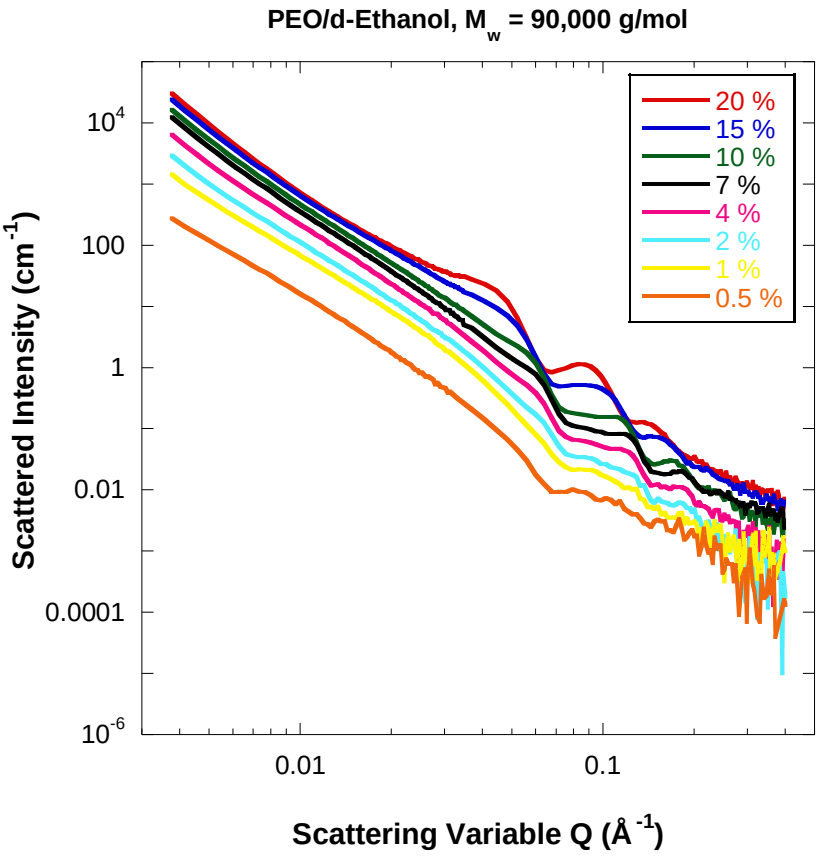

Figure 2: SANS data from PEO/d-ethanol for the various mass fractions measured. Measurements were taken at 23 ^{o}C, i.e., well into the crystalline region. The incoherent background component has been subtracted.

In order to discriminate among the various effects that could cause the strong low-Q signal, a couple of standard characterization methods are used. These methods can detect crystallization. The first method is Differential Scanning Calorimetry (DSC) which clearly shows a crystal melting process upon heating and a crystallization process upon cooling.

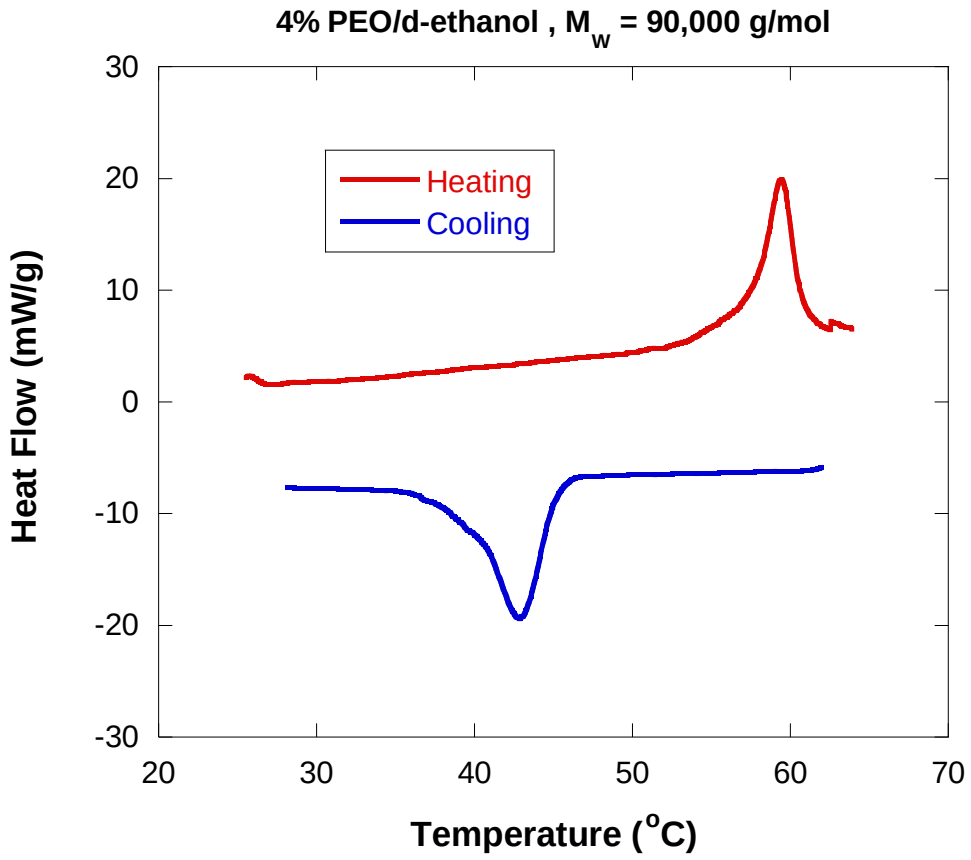

Figure 3: Differential Scanning Calorimetry (DSC) measurements from 4 % PEO/d-ethanol showing the crystalline nature. The heating and cooling curves show the effect of melting and crystallization.

The second good monitor of sample crystallization is Wide-Angle X-ray Scattering (WAXS). This method clearly shows crystalline peaks even at low PEO mass fraction.

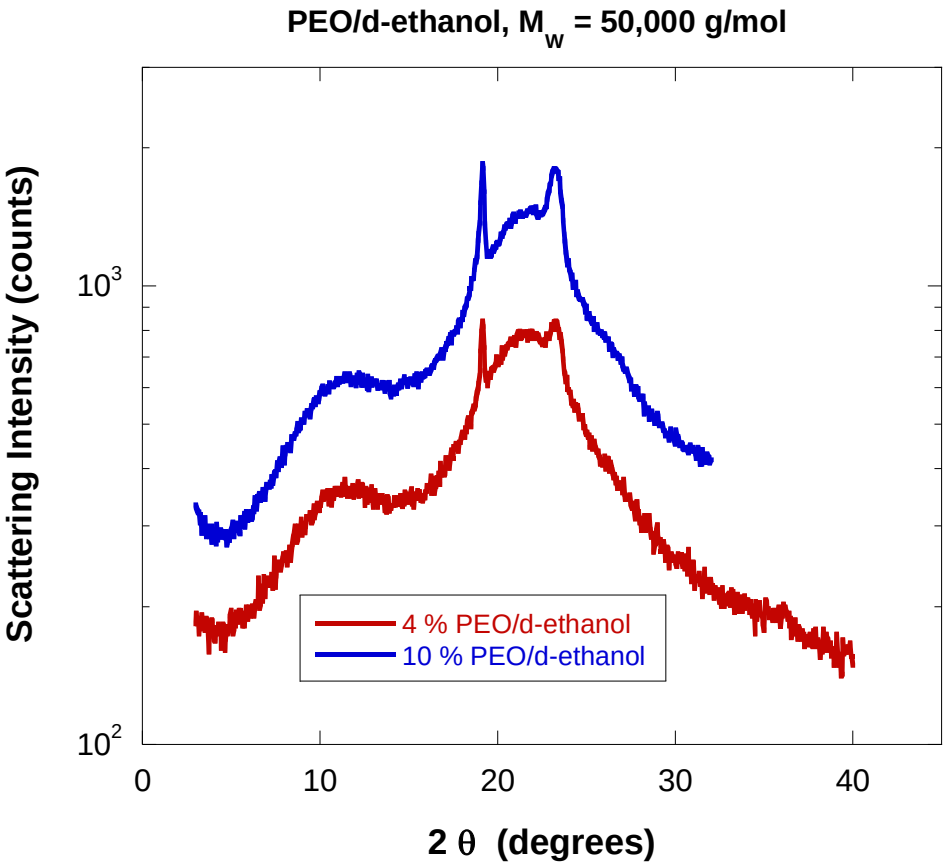

Figure 4: Wide-Angle X-ray Scattering (WAXS) spectra from PEO/ethanol showing crystallinity in the sample. Note that most of the spectrum consists of amorphous halos but two crystalline peaks are observed. The second spectrum was shifted upward.

Another method for determining crystal melting temperatures (while heating) and crystallization temperatures (while cooling) consists in precise density measurements.

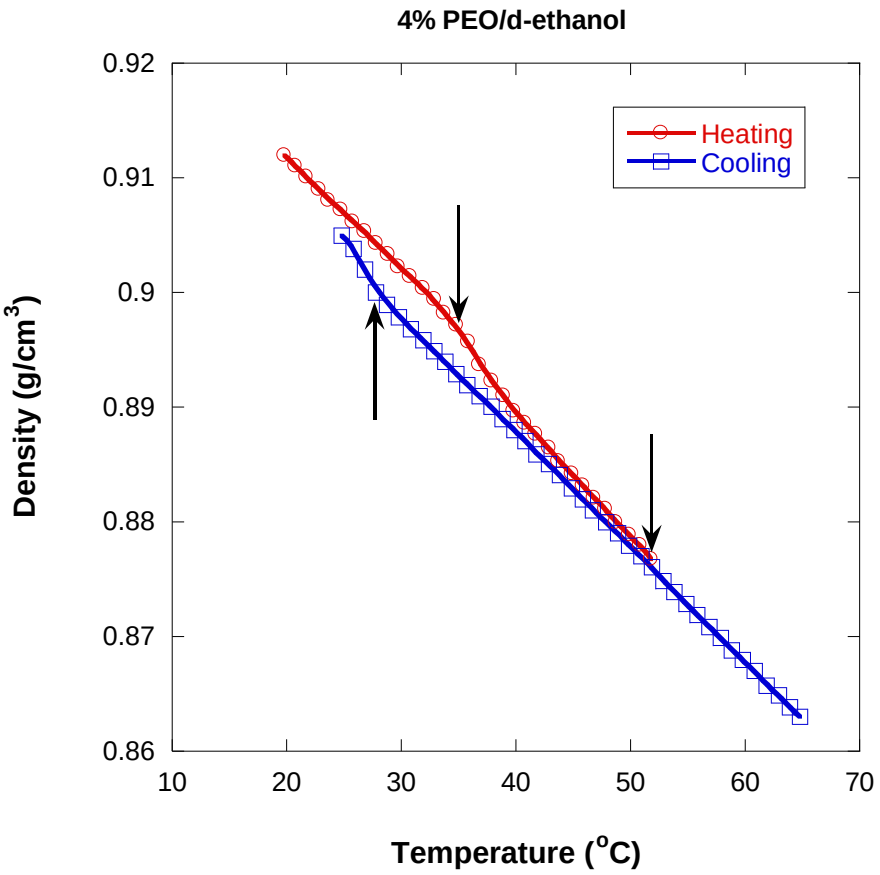

Figure 5: Density measurements for 4 % PEO/d-ethanol. The heating and cooling cycles are shown. Arrows show breaks in the data trend corresponding to melting and crystallization transitions.

2. CLUES ABOUT THE PEO/D-ETHANOL SYSTEM

PEO crystallizes in ethanol even at low mass fractions. Minutes after mixing PEO and ethanol, the solution turns white and gel-like; it does not flow when turned upside-down. When probed using a needle, the structure feels sponge-like. This structure could be referred to as a lamellar sponge.

In order to analyze the measured SANS data, the following model in used.

3. FORM FACTOR FOR A SINGLE LAMELLA

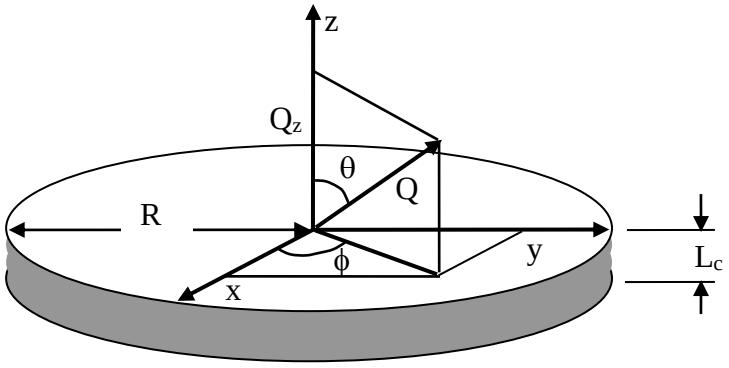

Figure 6: Coordinates parametrization of a single lamella.

The form factor amplitude F(Q,μ) for a single-lamella has two contributions: one for the Q component parallel to the z-axis and one in the horizontal plane.

$$F(Q,\mu) = F_z(Q,\mu)F_\perp(Q,\mu) \qquad (1)$$

$$F_z(Q,\mu) = \frac{1}{L_c}\int_{-L_c/2}^{L_c/2} dz \exp[-iQ\mu z] = \frac{\sin(Q\mu L_c/2)}{Q\mu L_c/2} \qquad (2)$$

$$F_\perp(Q,\mu) = \frac{1}{\pi R^2}\int_0^R d\rho\rho\int_0^{2\pi} d\phi \exp[-iQ\sqrt{1-\mu^2}\cos(\phi)\rho]\,. \qquad (3)$$

Here μ = cos(θ) and θ is the inclination angle. After manipulations described elsewhere, one obtains:

$$F_\perp(Q,\mu) = \frac{2J_1(Q\sqrt{1-\mu^2}R)}{Q\sqrt{1-\mu^2}R}. \qquad (4)$$

J_1 is the cylindrical Bessel function. The final result for the form factor amplitude for a single lamella is:

$$F(Q,\mu) = \left[\frac{\sin(Q\mu L_c/2)}{Q\mu L_c/2}\right]\left[\frac{2J_1(Q\sqrt{1-\mu^2}R)}{Q\sqrt{1-\mu^2}R}\right]. \qquad (5)$$

The form factor for a single isolated lamella is therefore given by the following orientational average:

$$P(Q) = \frac{1}{2}\int_{-1}^{1} d\mu \,|\, F(Q,\mu)\,|^2 . \qquad (6)$$

Lamellae form in stacks. Here, the lamellae are not isolated so that the orientational averaging is not performed until the inter-lamellae stack structure factor is included.

4. INTER-LAMELLAE STRUCTURE FACTOR

Consider a stack of N lamellae consisting of alternating crystalline and amorphous regions. L is the inter-lamellar distance (also called long period), L_C is the lamella thickness and R is the radius (Richter et al, 1997; Ho et al, 2006).

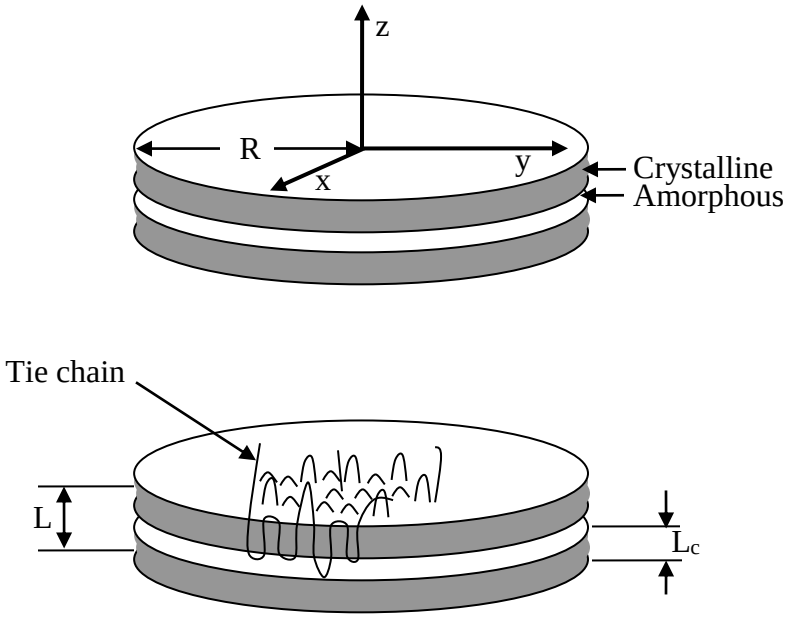

Figure 7: Stack of multiple lamellae.

Consider the following inter-lamellae Gaussian distribution function:

$$W_k(z,L) = \frac{1}{\sqrt{2\pi k\sigma_L{}^2}} \exp\left[-\frac{(z-kL)^2}{2k\sigma_L{}^2}\right]. \qquad (7)$$

Note that the variance $k\sigma_L^2$ gets larger and the Gaussian peak height gets smaller with increasing lamellar order k within a stack.

The structure factor for a stack of N lamellae is given by:

$$S_I(Q,\mu) = \frac{1}{N^2}\sum_{i,j=0}^{N} < \exp[-iQ\mu z] > \qquad (8)$$

$$= \frac{1}{N^2}\sum_{i,j=0}^{N}\frac{1}{L}\int dz \exp[-iQ\mu z] W_{|i-j|}(z,L).$$

Here $Q_z = Q\mu$ is the projection along the vertical (z) axis and the "I" subscript on the structure factor stands for "inter-lamellae". The z integration is readily performed:

$$\frac{1}{L}\int dz \frac{\exp[-iQ\mu z]}{\sqrt{2\pi |i-j| {\sigma_L}^2}} \exp\left[-\frac{(z-|i-j|L)^2}{2|i-j|{\sigma_L}^2}\right] = \exp[-iQ\mu |i-j| L]\exp\left[-\frac{Q^2\mu^2 |i-j| {\sigma_L}^2}{2}\right] \qquad (9)$$

Use the following summation identity:

$$\sum_{i,j=1}^{N} F(|i-j|) = N + 2\sum_{k=1}^{N}(N-k)F(k). \qquad (10)$$

to obtain:

$$S_I(Q,\mu) = \frac{1}{N} + \frac{2}{N^2}\sum_{k=1}^{N}(N-k)\exp[-iQ\mu kL]\exp\left[-\frac{Q^2\mu^2 k{\sigma_L}^2}{2}\right]. \qquad (11)$$

This result is general and applies for a finite stack of lamellae.

Note that the hypothetical (unrealistic) case where L = 0 yields the following familiar function:

$$S_I(Q,\mu) = \frac{1}{N} + 2\left[\frac{\exp(-A)-1+A}{A^2}\right]. \qquad (12)$$

This is the Debye function encountered when calculating the form factor for a Gaussian coil and the variable is $A = Q^2\mu^2{\sigma_L}^2/2$. These two widely different systems involve the same function by mere coincidence.

The infinite stack case is obtained by taking the $N \to \infty$ limit. The following result is obtained:

$$S_I(Q,\mu) = \frac{1}{N} + \frac{\exp(Q^2\mu^2{\sigma_L}^2/2) - \exp(-Q^2\mu^2{\sigma_L}^2/2)}{\exp(Q^2\mu^2{\sigma_L}^2/2) + \exp(-Q^2\mu^2{\sigma_L}^2/2) - 2\cos(Q\mu L)} \qquad (13)$$

$$S_I(Q,\mu) = \frac{1}{N} + \frac{\sinh(Q^2\mu^2{\sigma_L}^2/2)}{\cosh(Q^2\mu^2{\sigma_L}^2/2) - \cos(Q\mu L)}.$$

This is a more compact result but applies only for stacks with infinite number of lamellae.

5. THE SCATTERING FACTOR

Putting the single-lamella form factor and the inter-lamella structure factor together gives the following scattering factor:

$$\frac{1}{2}\int_{-1}^{1} d\mu P(Q,\mu) S_I(Q,\mu) \qquad (14)$$

$$\frac{1}{2}\int_{-1}^{1} d\mu \left[\frac{\sin(Q\mu L_c/2)}{Q\mu L_c/2}\right]^2 \left[\frac{2J_1(Q\sqrt{1-\mu^2}R)}{Q\sqrt{1-\mu^2}R}\right]^2 S_I(Q,\mu).$$

This model assumes uniform crystalline density within each lamella and neglects completely scattering from the amorphous phase between the lamellae. Note that in writing down this scattering factor, we did not worry too much about normalization factors. These factors are included in the next section where the scattering cross section is written down.

6. THE STACKED LAMELLAE MODEL

Consider a scattering system consisting of a sponge-like structure where the lamellae trap solvent. A few lamellae packed into stacks form the partitions. Each stack contains a number of crystalline lamellae and amorphous regions in-between the lamellae. Solvent dissolves the amorphous regions and fills the pockets of the sponge-like structure. Note that the extent of the stack (its radius) is not well-defined. It is large and could be thought of as the average distance between bifurcation points.

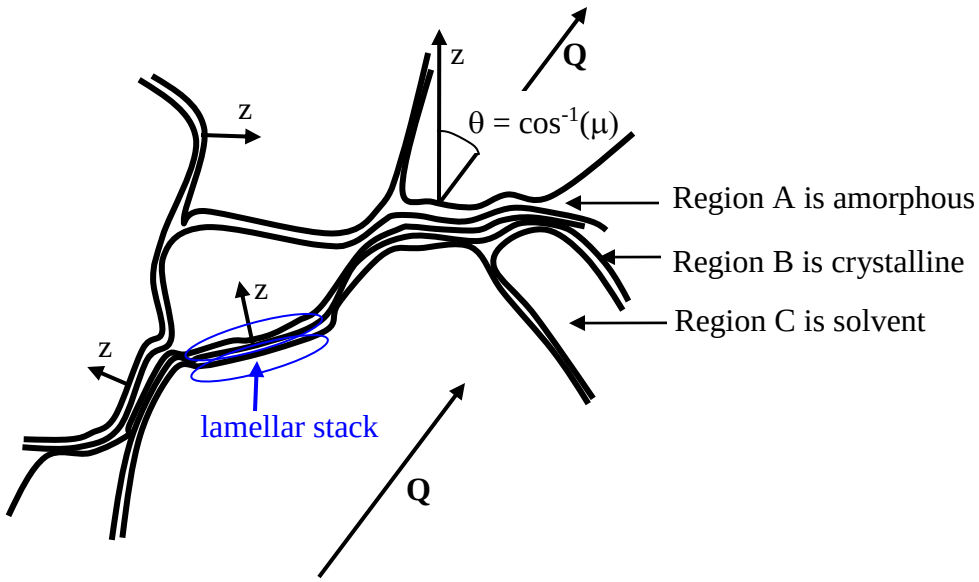

Figure 8: The stacked lamellae model consists of alternating amorphous and crystalline regions that surround solvent pockets.

The following parameters are used in the model.

L_A: thickness of the amorphous region
L_B: thickness of the crystalline region
L: lamellar spacing ($L = L_A+L_B$)
N: number of lamellae per stack
σ_L: standard deviation of lamellar spacing
$V_A = \pi R^2 L_A$: volume of one amorphous region
$V_B = \pi R^2 L_B$: volume of one crystalline region
R: average radius of the lamellar stack
$V_{A+B} = \pi R^2 L$: volume of one crystalline and one amorphous regions
$\rho_A = b_A/v_A$: scattering length density of the amorphous region (region A)
$\rho_B = b_B/v_B$: scattering length density of the crystalline region (region B)
$\rho_C = b_C/v_C$: scattering length density of the solvent region (region C)
N_S/V: lamellar stacks number density.

The orientation-dependent cross section is given by:

$$\left[\frac{d\Sigma(Q,\mu)}{d\Omega}\right] = \left(\frac{\phi_S}{V_S}\right)\left[\left(\frac{b_A}{v_A}-\frac{b_C}{v_C}\right)V_A F_A(Q,\mu)+\left(\frac{b_B}{v_B}-\frac{b_C}{v_C}\right)\left[V_{A+B}\,F_{AB}(Q,\mu)-V_A F_A(Q,\mu)\right]\right]^2 S_I(Q,\mu) \tag{15}$$

$$\left[\frac{d\Sigma(Q,\mu)}{d\Omega}\right] = \left(\frac{\phi_S}{V_S}\right)\left[\left(\frac{b_A}{v_A}-\frac{b_B}{v_B}\right)V_A F_A(Q,\mu)+\left(\frac{b_B}{v_B}-\frac{b_C}{v_C}\right)V_{A+B}\,F_{AB}(Q,\mu)\right]^2 S_I(Q,\mu).$$

Note that the number density of the lamellar stacks N_S/V has been expressed in terms of the stacks volume fraction ϕ_S and stack volume V_S as $N_S/V = \phi_S/V_S$.

The form factors are:

$$F_A(Q,\mu) = \left[\frac{\sin(Q\mu L_A/2)}{Q\mu L_A/2}\right]\left[\frac{2J_1(Q\sqrt{1-\mu^2}R)}{Q\sqrt{1-\mu^2}R}\right] \qquad (16)$$

$$F_{AB}(Q,\mu) = \left[\frac{\sin(Q\mu L/2)}{Q\mu L/2}\right]\left[\frac{2J_1(Q\sqrt{1-\mu^2}R)}{Q\sqrt{1-\mu^2}R}\right].$$

The inter-lamellae structure factor for each stack is given by:

$$S_I(Q,\mu) = \frac{1}{N} + \frac{2}{N^2}\sum_{k=1}^{N}(N-k)\exp[iQ\mu kL]\exp\left[-\frac{Q^2\mu^2 k\sigma_L^{\,2}}{2}\right]. \qquad (17)$$

The orientationally averaged cross section is obtained as:

$$\frac{d\Sigma(Q)}{d\Omega} = \frac{1}{2}\int_{-1}^{1} d\mu \frac{d\Sigma(Q,\mu)}{d\Omega}. \qquad (18)$$

The scattering intensity consists of the following contributions:

$$I(Q) = \frac{A}{Q^n} + \frac{d\Sigma(Q)}{d\Omega} + B. \qquad (19)$$

The lamellar stacks represent only the crystalline-amorphous regions forming the walls of the sponge-like structure. Scattering comprises also scattering from the sponge-like structure itself. A term A/Q^n term has been added to represent the lamellar non-stack scattering component. This component has contributions from the clustering network of the sponge-like structure (mass fractal network and surface fractal lamellae). B is a Q-independent (mostly incoherent) scattering background.

7. MODEL FITTING

The stacked lamellae model is smeared with the instrumental resolution function and used to fit SANS data from PEO/d-ethanol samples in the crystalline region.

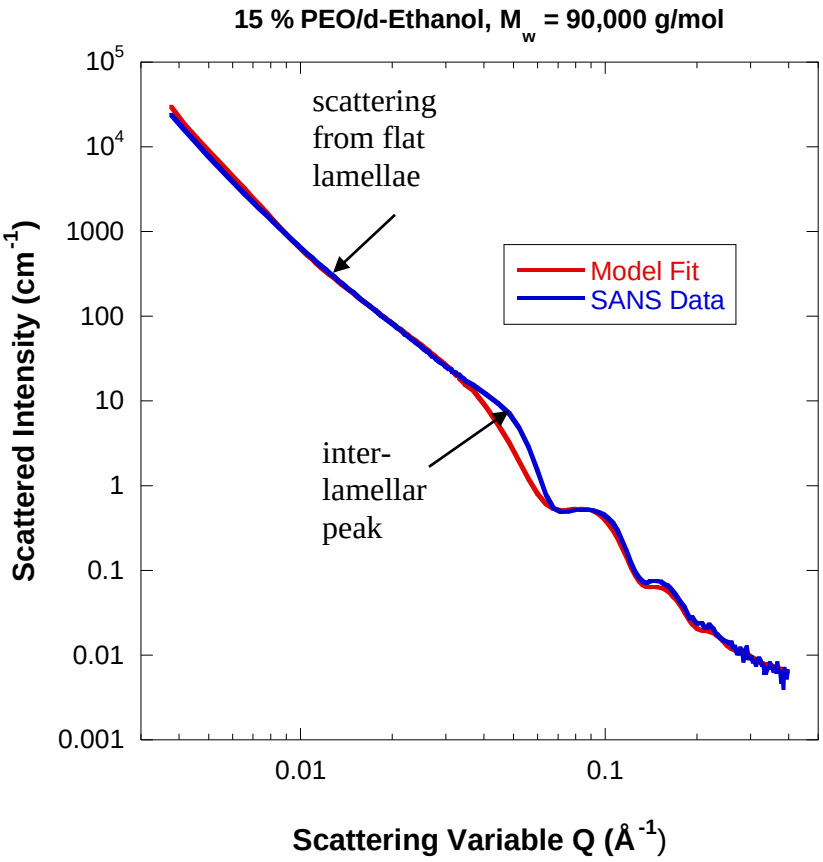

Figure 9: Comparison of the SANS data and the stacked lamellae smeared model for the 15 % PEO/d-ethanol sample at 23 ºC. The model fits the data fairly well except for a region in the middle of the window.

Results of the fit follow.

Lamellar stacks volume fraction $\phi_S = 0.36$
Lamellae radius R = 10,757 Å
Thickness of the amorphous region $L_A = 3$ Å
Lamellar thickness $L_B = 50$ Å
Scattering length density of the amorphous region $\rho_A = 4.15*10^{-6}$ Å^{-2}
Scattering length density of the crystalline region $\rho_B = 7.67*10^{-7}$ Å^{-2}
Scattering length density of the d-ethanol solvent region $\rho_S = 6.07*10^{-6}$ Å^{-2}
Number of lamellae per stack $N_L = 6.86$
Standard deviation of the inter-lamellar distance $\sigma_L = 0.56$ Å
Clustering scaling factor $A = 282*10^{-6}$ cm^{-1}
Clustering Porod exponent n = 2.8
Constant (incoherent) background level B = 0.004 cm^{-1}.

The solvent scattering length density ρ_S was fixed. All other 11 fitting parameters were varied. With so many varying parameters, it is difficult to find a unique solution. The one

presented here gives an idea of the magnitude of the various parameters. Constraints such as ordering the various scattering length densities as $\rho_{EO} < \rho_B < \rho_A < \rho_{dEth}$ help the fitting.

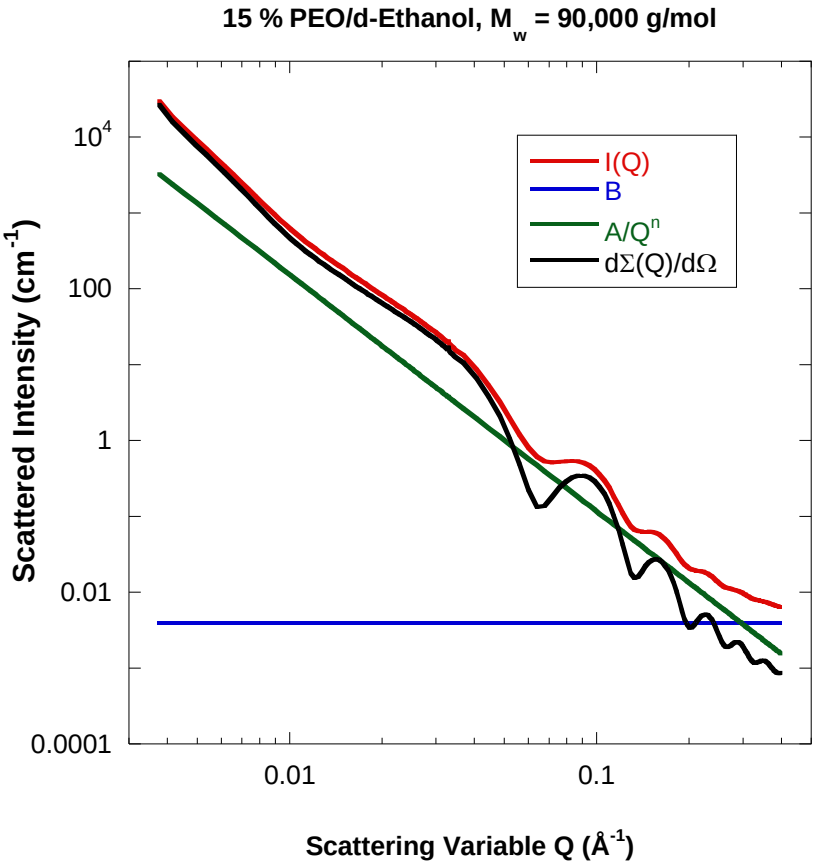

Figure 10: Breakdown of the various terms forming the fitting model functional form. Note that $I(Q) = d\Sigma(Q)/d\Omega + A/Q^n + B$.

8. THE MATERIAL BALANCE EQUATIONS

Consider a solution consisting of lamellar stacks comprising alternating amorphous and crystalline regions. We assume that D_2O exists in the amorphous and crystalline regions; i.e., that there are y_A d-ethanol molecules per ethylene oxide (EO) monomer in the amorphous region (region A) and y_B d-ethanol molecules per EO monomer in the crystalline region (region B). Note that most of the solvent exists in the sponge-like pockets outside of the lamellar stacks. Define N_{agg} as the aggregation number, i.e., the number of PEO macromolecules per lamellar stack and note that there are n EO monomers per macromolecule. These are distributed as $n_A = nf_A$ monomers in region A and $n_B = nf_B$ in region B.

The fitting parameters are L_A, L_B, ρ_A, ρ_B, R, N_L, and σ_L. Other known quantities are the specific volumes v_{EO}^A (EO in the amorphous region), v_{EO}^B (EO in the crystalline region)

and v_{dEth} and the scattering lengths b_{EO} and b_{dEth}. The unknown parameters are y_A, y_B, f_A, and N_{ag}. Note that $f_B = 1\text{-}f_A$.

The material balance equations are:

$$(1)\ \pi L_A R^2 N_L = N_{ag} f_A n \left(v_{EO}^A + v_{dEth} y_A\right) \qquad (20)$$

$$(2)\ \pi L_B R^2 N_L = N_{ag} f_B n \left(v_{EO}^B + v_{dEth} y_B\right)$$

$$(3)\ \rho_A = \frac{N_{ag} f_A n\left(b_{EO} + b_{dEth} y_A\right)}{4\pi L_A R^2 N_L}$$

$$(4)\ \rho_B = \frac{N_{ag} f_B n\left(b_{EO} + b_{dEth} y_B\right)}{4\pi L_B R^2 N_L}\ .$$

These four linear equations can be solved to obtain:

$$y_A = \frac{\rho_A v_{EO}^A - b_{EO}}{b_{dEth} - \rho_A v_{dEth}} \qquad (21)$$

$$y_B = \frac{\rho_B v_{EO}^B - b_{EO}}{b_{dEth} - \rho_B v_{dEth}}$$

$$f_A = \frac{\left(v_{EO}^B + y_B v_{dEth}\right)\frac{L_A}{L_B}}{\left(v_{EO}^A + y_A v_{dEth}\right) + \left(v_{EO}^B + y_B v_{dEth}\right)\frac{L_A}{L_B}}$$

$$f_B = 1 - f_A$$

$$N_{ag} = \frac{4\pi R^2 L_A N_L}{n f_A \left(v_{EO}^A + y_A v_{dEth}\right)}.$$

We have transformed the four fitting parameters L_A, L_B, ρ_A and ρ_B into four meaningful parameters y_A, y_B, f_A and N_{ag}. This set of solutions is unique. Note that only N_{ag} depends on the ill-defined stack radius R.

9. NUMERICAL APPLICATION

Consider the PEO/d-ethanol system described earlier. Some of the known parameters follow:

$$v_{EO}^{A} = 42.82\,cm^3/mol \qquad (23)$$
$$v_{EO}^{B} = 38.93\,cm^3/mol$$
$$v_{dEth} = 58.56\,cm^3/mol$$
$$b_{EO} = 4.14*10^{-13}cm$$
$$b_{dEth} = 59.12*10^{-13}cm\,.$$

Note that the amorphous region's specific volume has been taken to be 10 % higher than that for the crystalline region. Using these parameters along with the following fitting parameters:

ϕ_S = 0.36 (24)
R = 10,757 Å
L_A = 3 Å
L_B = 50 Å
$\rho_A = 4.15*10^{-6}$ Å^{-2}
$\rho_B = 7.67*10^{-7}$ Å^{-2}
$\rho_S = 6.07*10^{-6}$ Å^{-2}
N_L = 6.86
σ_L= 0.56 Å.

The material balance equations yield:

y_A = 3.7 (25)
y_B = 0.02
f_A = 0.01
f_B = 0.99
N_{ag} = 926,000

Fit results yield 3.7 solvent molecules per EO monomer in the amorphous region and no solvent in the crystalline region. Moreover, most of the EO monomers are found in the crystalline regions.

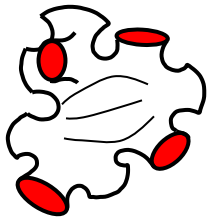

Figure 11: Schematic representation of the sponge-like structure. The sponge walls are formed of lamellar stacks that trap pockets of solvent.

In order to acquire a “picture” of the sponge-like structure in direct space, TEM was performed. A micrograph is included.

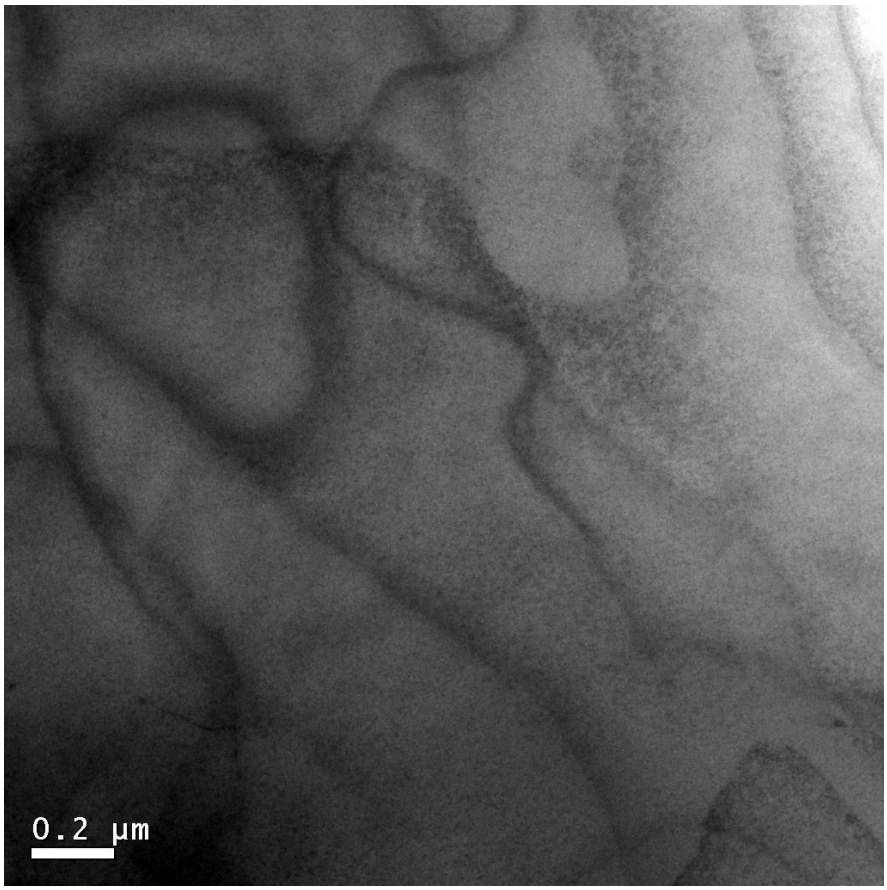

Figure 12: Transmission Electron Micrograph (TEM) of a 4 % PEO/ethanol crystalline sample. The sample was stained. The sponge-like crystalline structure traps pockets of solvent.

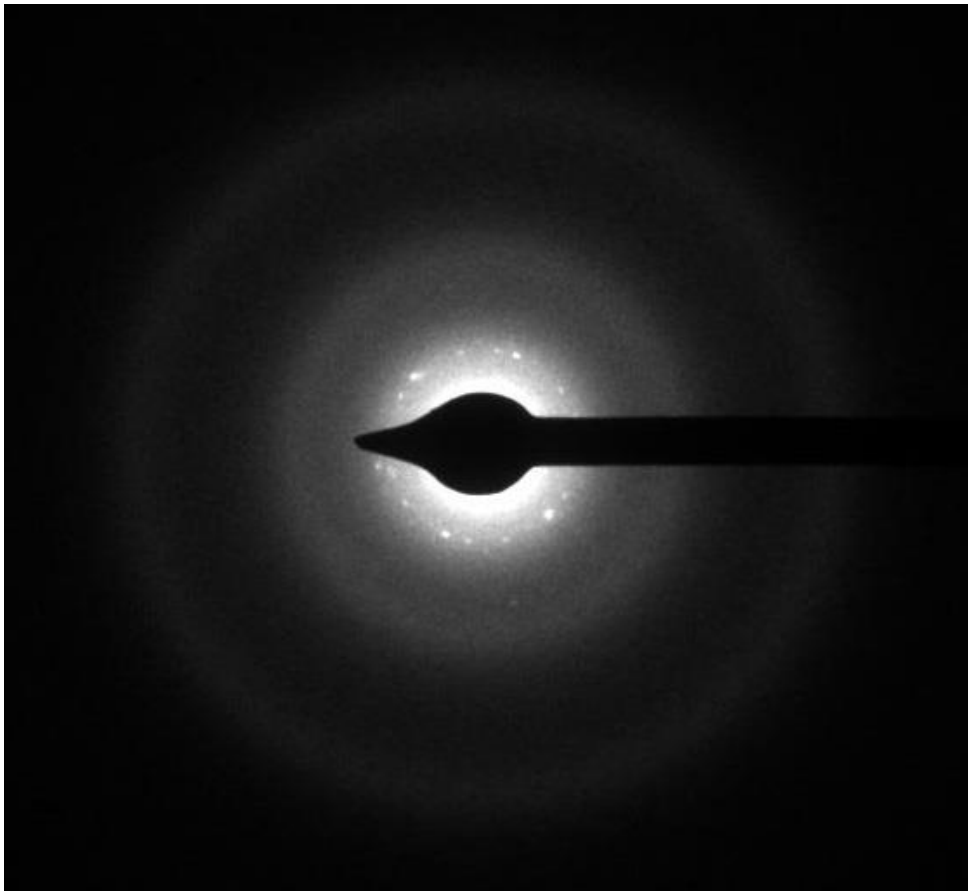

Figure 13: Electron diffraction micrograph from the same 4 % PEO/ethanol semicrystalline sample. The diffraction spectrum shows strong low-Q scattering and a series of peaks forming a ring at Q = 0.05 $Å^{-1}$.

The exercise described here gives an idea of what it takes to understand some SANS data: clues about the sample, model fitting and a great deal of common sense.

REFERENCES

D. Richter, D. Schneiders, M. Monkenbush, L. Willner, L.J. Fetters, J.S. Huang, M. Lin, K. Mortensen and B. Farago, "Polymer Aggregates with Crystalline Cores: The System Polyethylene-Poly(ethylenepropylene)", Macromolecules 30, 1053-1068 (1997).

D.L Ho, B. Hammouda, S.R. Kline and W-R Chen, "Unusual Phase Behavior in Mixtures of Poly(ethylene oxide) and Ethyl Alcohol", J. Polym. Sci., Polym. Phys. Ed. 55, 557-564 (2006)

QUESTIONS

1. Crystalline lamellar morphology is formed in what conditions?
2. What are the main pieces used to work out the scattering from a lamellar system?
3. Why is the scattering from crystalline lamellae characterized by SANS oscillations at high-Q?
4. Why is the inter-lamellae scattering (also called long period) characterized by a Bragg peak?
5. Lamellar growth occurs either following the "adjacent" or the "random switchboard" re-entry. Which occurs in solution crystallization and which occurs in melt crystallization?
6. Are the crystallization and the crystal melting temperatures the same? Which is lower? Why?

ANSWERS

1. Crystalline polymers form lamellar morphology in solution as well as in the melt state. In the melt state, however, lamellae organize into spherulitic structures.
2. Scattering from a lamellar system is calculated using the form factor for a lamella and the inter-lamellar structure factor.
3. SANS scattering from crystalline lamellae is characterized by oscillations at high-Q because of the sharp (highly monodisperse) lamellar size.
4. The inter-lamellae scattering is characterized by a Bragg peak because of the well-defined characteristic d-spacing between lamellae.
5. Adjacent re-entry occurs in solution crystallization and random switchboard occurs in melt crystallization. This is due to the slower crystalline growth kinetics in solution crystallization.
6. Crystallization is obtained through cooling whereas crystal melting happens though heating. For this, the crystallization temperature is lower than the melting temperature due to the "hysteresis" effect. This effect is seen on the DSC spectra included earlier.